RESEARCH ARTICLE

REVISED [2.2.2.2]Paracyclophanetetraenes (PCTs): cyclic structural analogues of poly(*p*-phenylene vinylene)s (PPVs) [version 2; peer review: 2 approved]

Matthias Pletzer[1,2], Felix Plasser[3], Martina Rimmele[1,2], Martin Heeney[1,2], Florian Glöcklhofer[1,2]

[1]Department of Chemistry, Imperial College London, London, W12 0BZ, UK
[2]Centre for Processable Electronics, Imperial College London, London, W12 0BZ, UK
[3]Department of Chemistry, Loughborough University, Loughborough, LE11 3TU, UK

v2 **First published:** 23 Sep 2021, **1**:111
https://doi.org/10.12688/openreseurope.13723.1
Latest published: 10 Mar 2022, **1**:111
https://doi.org/10.12688/openreseurope.13723.2

Abstract

Background: Poly(*p*-phenylene vinylene)s (**PPV**s) and [2.2.2.2]paracyclophanetetraene (**PCT**) are both composed of alternating π-conjugated *para*-phenylene and vinylene units. However, while the former constitute a class of π-conjugated polymers that has been used in organic electronics for decades, the latter is a macrocycle that only recently revealed its potential for applications such as organic battery electrodes. The cyclic structure endows **PCT** with unusual properties, and further tuning of these may be required for specific applications. **Methods**: In this article, we adopt an approach often used for tuning the properties of **PPV**s, the introduction of alkoxy (or alkylthio) substituents at the phenylene units, for tuning the optoelectronic properties of **PCT**. The resulting methoxy- and methylthio-substituted **PCT**s, obtained by Wittig cyclisation reactions, are studied by UV-vis absorption, photoluminescence, and cyclic voltammetry measurements, and investigated computationally using the visualisation of chemical shielding tensors (VIST) method. **Results**: The measurements show that substitution leads to slight changes in terms of absorption/emission energies and redox potentials while having a pronounced effect on the photoluminescence intensity. The computations show the effect of the substituents on the ring currents and chemical shielding and on the associated local and global (anti)aromaticity of the macrocycles, highlighting the interplay of local and global aromaticity in various electronic states. **Conclusions**: The study offers interesting insights into the tuneability of the properties of this versatile class of π-conjugated macrocycles.

Open Peer Review

Approval Status ✓ ✓

	1	2
version 2 (revision) 10 Mar 2022		✓ view
version 1 23 Sep 2021	✓ view	? view

1. **Weixuan Zeng**, University of Cambridge, Cambridge, UK

2. **Miłosz Pawlicki**, Jagiellonian University, Kraków, Poland

Any reports and responses or comments on the article can be found at the end of the article.

Keywords
macrocycles, π-conjugated macrocycles, paracyclophanetetraene, PCT, poly(p-phenylene vinylene), PPV, visualisation of chemical shielding tensors, VIST, aromaticity, antiaromaticity, rotamers, Wittig reaction, photoluminescence, cyclic voltammery

This article is included in the Excellent Science gateway.

This article is included in the Redox Reactions collection.

Corresponding author: Florian Glöcklhofer (f.glocklhofer@imperial.ac.uk)

Author roles: Pletzer M: Investigation, Methodology, Validation, Writing – Original Draft Preparation, Writing – Review & Editing; **Plasser F**: Data Curation, Formal Analysis, Funding Acquisition, Investigation, Methodology, Project Administration, Resources, Validation, Visualization, Writing – Original Draft Preparation, Writing – Review & Editing; **Rimmele M**: Investigation, Validation; **Heeney M**: Funding Acquisition, Project Administration, Supervision, Writing – Review & Editing; **Glöcklhofer F**: Conceptualization, Data Curation, Funding Acquisition, Methodology, Project Administration, Resources, Supervision, Visualization, Writing – Original Draft Preparation, Writing – Review & Editing

Competing interests: No competing interests were disclosed.

Grant information: This research was financially supported by the European Union's Horizon 2020 research and innovation programme under the Marie Skłodowska-Curie grant agreement No 796024. This work was also supported by funding from the Austrian Science Fund (FWF), project number J 4463, and from the Engineering and Physical Sciences Research Council (EPSRC), grant EP/V048686/1.
The funders had no role in study design, data collection and analysis, decision to publish, or preparation of the manuscript.

How to cite this article: Pletzer M, Plasser F, Rimmele M *et al.* **[2.2.2.2]Paracyclophanetetraenes (PCTs): cyclic structural analogues of poly(*p*-phenylene vinylene)s (PPVs) [version 2; peer review: 2 approved]** Open Research Europe 2022, **1**:111 https://doi.org/10.12688/openreseurope.13723.2

First published: 23 Sep 2021, **1**:111 https://doi.org/10.12688/openreseurope.13723.1

REVISED **Amendments from Version 1**

In response to the reviewers' comments, photoluminescence quantum yields (PLQYs) of the investigated macrocycles were determined and the results were added in this updated version of the article. Furthermore, computations on O-PCT and S-PCT based on a frozen PCT structure were performed and a discussion of the results was added. The results are also presented in the newly added Table 1. The conclusions and methods sections as well as the provided underlying research data were updated to reflect these additions.

Any further responses from the reviewers can be found at the end of the article

Introduction

Poly(*p*-phenylene vinylene)s (**PPV**s) are among the best investigated π-conjugated polymers[1,2]. They are composed of alternating *para*-phenylene and vinylene units and usually feature substituents attached to the π-conjugated backbone to modify their optoelectronic and dissolution properties. Most frequently, alkoxy substituents are attached to the phenylene units, but the corresponding alkylthio-substituted **PPV**s have also been reported[3]. The alkyl part of the substituents (often a linear or branched alkyl chain) is intended to improve the solubility, while the purpose of the oxygen or sulfur atom linking the alkyl part to the backbone is to modify the optoelectronic properties, mainly through their positive mesomeric effect.

[2.2.2.2]Paracyclophanetetraene (**PCT**) can be seen as a cyclic structural analogue of unsubstituted **PPV** (Figure 1). This π-conjugated macrocycle, first synthesized in the 1970s[4], was recently rediscovered by us and has proven to be a capable battery electrode material[5]. The excellent redox and charge storage properties of **PCT** have been attributed to ring currents and voids enabled by the cyclic structure of the molecule, suggesting that the optoelectronic properties of **PCT** and **PPV** differ significantly, despite their structural similarity. In contrast to the polymers, the vinylene units in **PCT** must adopt a *cis*-configuration; no end groups are present that may affect the properties.

The aim of the work presented here was to synthesize and study **PCT** derivatives with alkoxy and alkylthio substituents at the phenylene units, in analogy to the well-investigated substituted **PPV**s. In contrast to **PPV**, **PCT** dissolves well in organic solvents also without substituents with linear or branched alkyl chains. Thus, simple methyl groups were selected as the alkyl part of the substituents. When studying the properties of the resulting methoxy- and methylthio-substituted **PCT** derivatives, we were particularly interested in the effect of the substituents on the ring currents, having recently reported the drastic effects of the introduction of ester groups (at the vinylene units) on these currents[6].

Results and discussion

Synthesis

Unsubstituted **PCT** can be synthesized by a Wittig cyclisation reaction in yields of 10% to 15% using [1,4-phenylenebis(methylene)]bis(triphenylphosphonium) dibromide (**P1**) and terephthalaldehyde (**P2**) as the cyclisation precursors[4,5]. Aiming for an analogous synthesis of methoxy- and methylthio-substituted **PCT** derivatives, we first synthesized the substituted Wittig cyclisation precursors **O-P1**, **S-P1**, and **S-P2** (Figure 2): The phosphonium salts **O-P1** and **S-P1** were synthesized via the same route, but while 1,4-dimethoxybenzene (**O-2**) for the synthesis of **O-P1** is readily available from commercial suppliers, the corresponding methylthio-substituted compound 1,4-bis(methylthio)benzene (**S-2**) for the synthesis of **S-P1** was obtained by a copper-catalysed conversion of 4-bromothioanisole (**S-1**) in dimethyl sulfoxide (DMSO)[7]. Compounds **O-2** and **S-2** were then bromomethylated by adapting our previously reported procedures to these substrates[3]. The reactions yielded

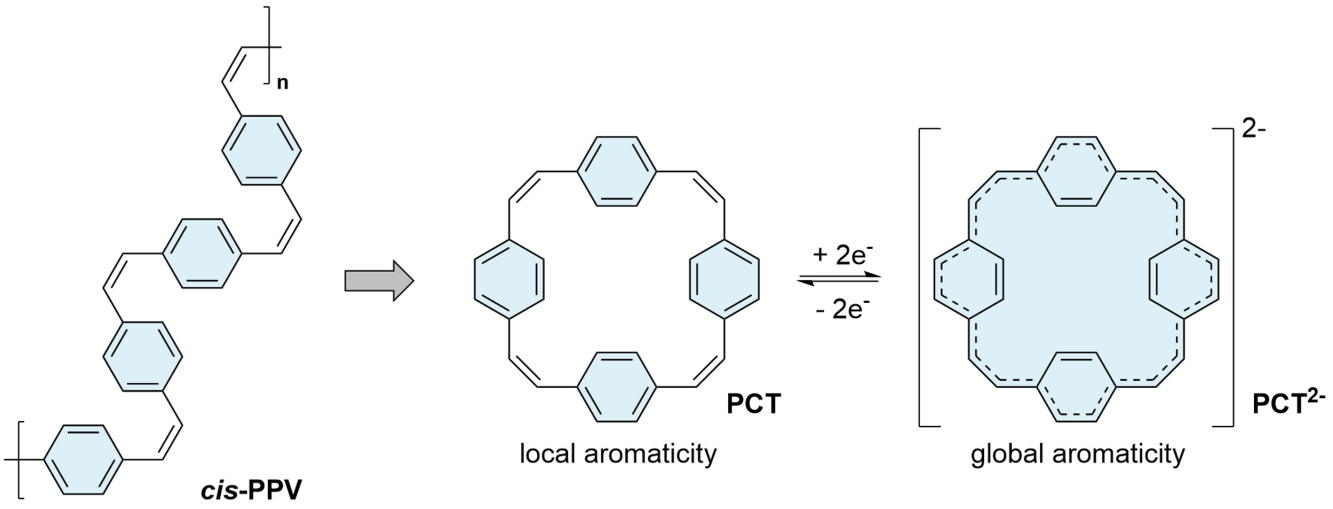

Figure 1. [2.2.2.2]Paracyclophanetetraene (PCT) as a cyclic structural analogue of *cis*-poly(*p*-phenylene vinylene) (*cis*-PPV) (left); reversible two-electron reduction and aromaticity switching of PCT (right).

compounds **O-3** and **S-3** in yields of 52% and 87%, respectively. In the final step, **O-3** and **S-3** were reacted with triphenylphosphine (PPh_3) in boiling toluene, affording **O-P1** and **S-P1** as white solids in good yields. In contrast, the dialdehyde **S-P2** was synthesized by slightly adapting published procedures for the bromination of **P2** in the first step and nucleophilic aromatic substitution with sodium methanethiolate ($NaSCH_3$) in the second step[8,9].

The phosphonium salts **O-P1** and **S-P1** were then reacted with terephthalaldehyde (**P2**) in dimethylformamide (DMF) at a low temperature of -40 °C (Figure 3). As for the synthesis of **PCT**[5], lithium methoxide dissolved in anhydrous methanol (MeOH) was used as the base for these Wittig cyclisation reactions. The base was added slowly using a syringe pump, affording the macrocycles **O-PCT** and **S-PCT** in yields of 9% and 14%, respectively, after work-up and purification by gel permeation chromatography (GPC). In contrast, placing the methylthio substituents on the aldehyde precursor instead of the phosphonium salt, reacting *p*-xylylenebis(triphenylphosphonium bromide) (**P1**) with precursor **S-P2** under the same reaction conditions, did not afford any **S-PCT**, presumably

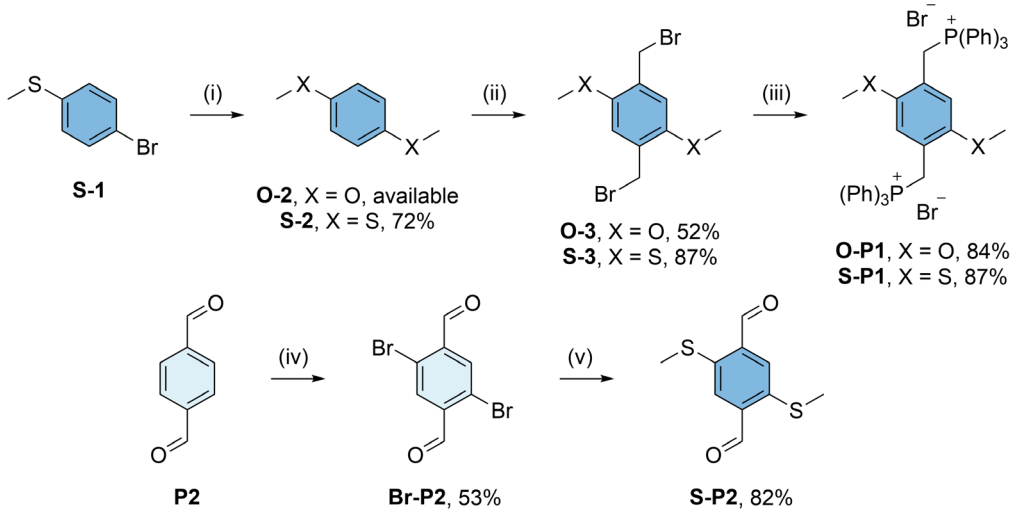

Figure 2. Synthesis of methoxy- and methylthio-substituted Wittig cyclisation precursors O-P1, S-P1, and S-P2. Reaction conditions: (i) CuI, $Cu(OAc)_2$, dimethyl sulfoxide (DMSO), 135 °C; (ii) paraformaldehyde, HBr in acetic acid, 1,4-dioxane (X = O) / formic acid (X = S), 80 °C; (iii) PPh_3, toluene, 120 °C; (iv) N-bromosuccinimide (NBS), conc. H_2SO_4, 60 °C; (v) $NaSCH_3$, dimethylformamide (DMF), r.t..

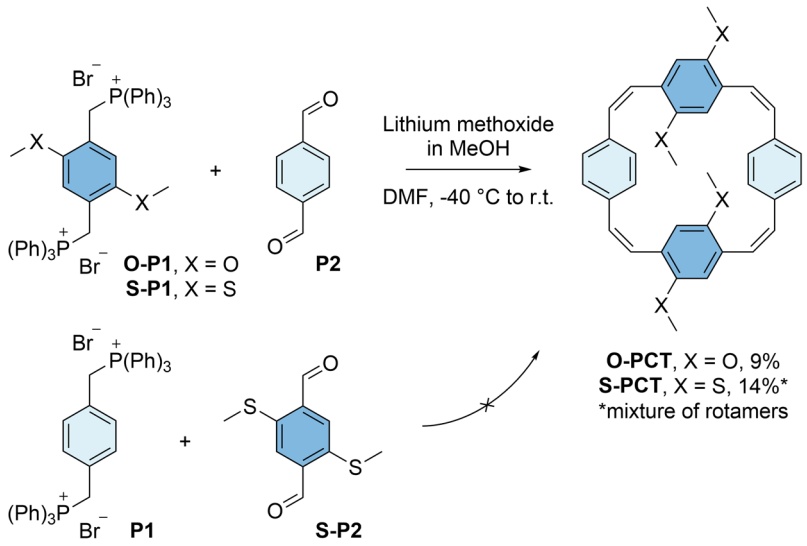

Figure 3. Synthesis of methoxy- and methylthio-substituted [2.2.2.2]paracyclophanetetraenes O-PCT and S-PCT by Wittig cyclisation reactions of precursors O-P1/S-P1 and P2 (top). The analogous reaction of precursors P1 and S-P2 did not yield the product (bottom).

due to a less favourable *cis*/*trans* ratio of the vinylene units formed in this Wittig reaction (the electronic character of the precursors can influence the ratio). The reaction of **S-P1** and **S-P2** to obtain the macrocycle with substituents on all four phenylene units has also been attempted but did not give the desired product.

Conformation

^{1}H NMR spectra of **S-PCT** recorded at room temperature and 50 °C indicated the presence of two rotamers that could not be separated (see Figure 4 for an illustration of the two rotamers). A rotamer ratio of approximately 10:1, which corresponds to a free energy difference of about 6 kJ/mol, was determined from the integrals. In contrast, the ^{1}H NMR spectrum of **O-PCT** did not show the presence of rotamers, indicating a lower energy barrier for the rotation of the phenylene units with methoxy substituents than with methylthio substituents.

To test these assumptions, computations were carried out to estimate the energy barrier for the interconversion of the two rotamers. Indeed, a barrier of only 45 kJ/mol was found for **O-PCT**. According to the Eyring equation, this corresponds to an interconversion time of about 10 µs, which is well below the time scale relevant to NMR. Both rotamers are very similar in energy, with the C_s rotamer 3.2 kJ/mol below the C_2 rotamer, suggesting that both are present at room temperature. **S-PCT**, on the other hand, showed a significantly enhanced barrier of 94 kJ/mol with an associated interconversion time well above one hour. The C_2 rotamer was found to be more stable by 16.6 kJ/mol, which is similar but somewhat larger than the free energy difference deduced from experiment (see above). The difference in behaviour between the two molecules can be understood by the fact that the methylthio groups are bulkier, causing steric strain for the transition state and the C_s rotamer. Taking the neutral C_2 rotamer as an example, we find that the two C-O bonds in **O-PCT** are 1.35 and 1.39 Å in length whereas the C-S bonds in **S-PCT** measure 1.77 and 1.81 Å.

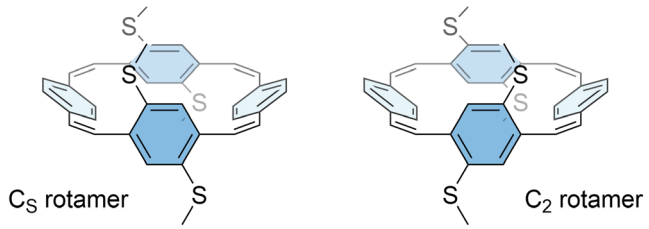

Figure 4. Illustration of the two rotamers of S-PCT, classified according to their idealised symmetry properties. The computed energy barrier for interconversion is 94 kJ/mol.

UV-vis absorption and photoluminescence

UV-vis absorption measurements in $CHCl_3$ solution (Figure 5, solid lines) showed slightly blueshifted absorption maxima for **O-PCT** ($\lambda_{abs,max}$ = 304 nm) and **S-PCT** ($\lambda_{abs,max}$ = 293 nm) compared to **PCT** ($\lambda_{abs,max}$ = 306 nm). The second absorption peak in the spectrum of **S-PCT** (λ_{abs} = 283 nm) may be attributed to the presence of two rotamers. Photoluminescence (PL) measurements of the solutions (Figure 5, dashed lines) showed a significant increase in PL intensity upon introduction of the substituents, particularly upon introduction of the methoxy substituents. Similar sensitivity to the substitution pattern for the PL intensity were also found for the related ester-substituted molecules and can be tentatively assigned to symmetry breaking in the excited state, lifting the selection rules for the formally symmetry-forbidden S_1 state[6], see, e.g., reference 10 for a discussion of the underlying physics. Despite the increase in PL intensity upon introduction of the substituents, all three macrocycles are still weak emitters, with a relative determination of the photoluminescence quantum yield (PLQY) indicating values of <1% for **O-PCT** and **S-PCT** and <0.1% for **PCT**. In contrast to the absorption maxima, the PL maxima of **O-PCT**

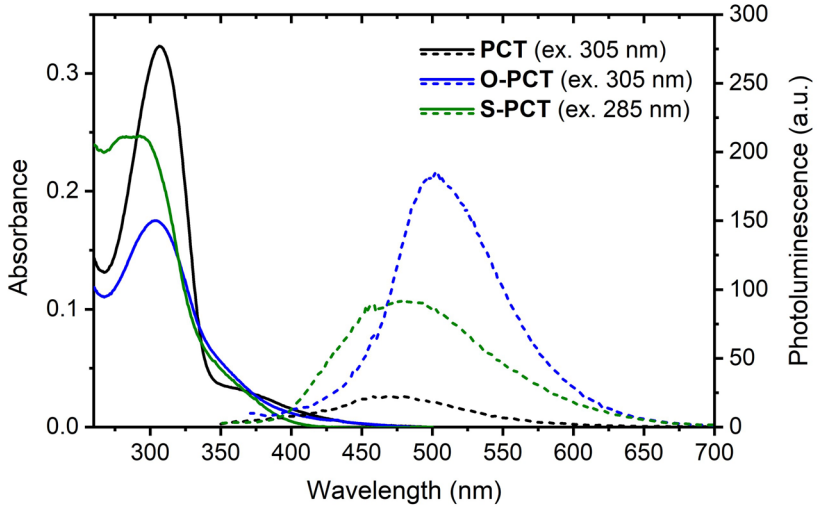

Figure 5. UV-vis absorption (solid lines) and photoluminescence spectra (dashed lines) of the macrocycles in $CHCl_3$ solution (5 µM). The excitation wavelengths for recording the photoluminescence (PL) spectra are shown in brackets.

($\lambda_{PL,max}$ = 502 nm) and **S-PCT** ($\lambda_{PL,max}$ = 481 nm) were found to be redshifted compared to **PCT** ($\lambda_{PL,max}$ = 468 nm), thus increasing their Stokes shifts from 1.40 eV for **PCT** to 1.61/1.65 eV for **O-PCT/S-PCT**. It is worth noting that the Stokes shifts of the linear **PCT** analogue containing 4 phenylene-vinylene units ($\lambda_{abs,max}$ = 396 nm; $\lambda_{PL,max}$ = 463 nm)[11], of alkoxy-substituted **PPV** ($\lambda_{abs,max}$ = 502 nm; $\lambda_{PL,max}$ = 558 nm)[12], and alkylthio-substituted **PPV** ($\lambda_{abs,max}$ = 453 nm; $\lambda_{PL,max}$ = 527 nm)[3] are all well below 0.5 eV, highlighting the dramatic effect of the cyclic conjugation. Indeed, the large Stokes shifts of the substituted and unsubstituted **PCT**s, resulting in almost no spectral overlap between absorption and emission, can be seen as a signature of excited-state aromaticity, *cf.* references 6 and 13. Thus, the spectra suggest that symmetry breaking is only a dynamic effect accounting for a minor perturbation of excited-state aromaticity (see below for a further discussion).

Redox potentials

Cyclic voltammetry measurements of the macrocycles in 1,2-dichloroethane (DCE) and dimethylformamide (DMF) (Figure 6) were carried out to determine the redox potentials *vs.* ferrocene/ferrocene$^+$ (Fc/Fc$^+$) in two different solvents. As a general trend, the redox potentials for both the reductions and oxidations shifted to lower values upon introduction of the substituents, with a slightly larger shift observed for the introduction of the methoxy substituents. This can be explained by the electron-donating character of the substituents.

In DCE, the redox potential for the first reduction wave shifted from -2.26 V for **PCT** to -2.34 V for **S-PCT** and -2.37 V for **O-PCT**. For **S-PCT**, a second reduction wave was observed at -2.50 V. The redox potential for the first oxidation wave shifted from 0.81 V for **PCT** to 0.73 V for **S-PCT** and 0.61 V for **O-PCT**. For **S-PCT**, the first derivative of the measurement indicated further oxidations at 0.79 V and 1.08 V. For **O-PCT**, a second and third oxidation wave were observed at 0.73 V and 1.03 V, respectively.

In DMF, the redox potential for the first reduction wave showed a shift from -2.09 V for **PCT** to -2.26 V for **S-PCT** and -2.27 V for **O-PCT**. No further reduction waves were observed in this solvent. The redox potential for the first oxidation wave shifted from 0.76 V for **PCT** to 0.62 V for **S-PCT** and 0.58 V for **O-PCT**. A second oxidation wave was observed at 0.83 V for **S-PCT** and 0.74 V for **O-PCT**.

Computations place the potentials for concerted two-electron reduction in DCE at -2.28, -2.40, and -2.35 V for **PCT**, **O-PCT**, and **S-PCT**, respectively, suggesting that the experimental reduction potentials refer to two-electron processes. Potentials for two-electron oxidation are placed at 0.89, 0.75, and 0.98 V for the three molecules. Considering that the values for **O-PCT** and **S-PCT** are considerably higher than the measured first oxidation potentials, this suggests that oxidation proceeds via one-electron processes.

Ring currents and chemical shielding

To study the effect of the methoxy and methylthio substituents on the magnetic properties (ring currents and chemical shielding)

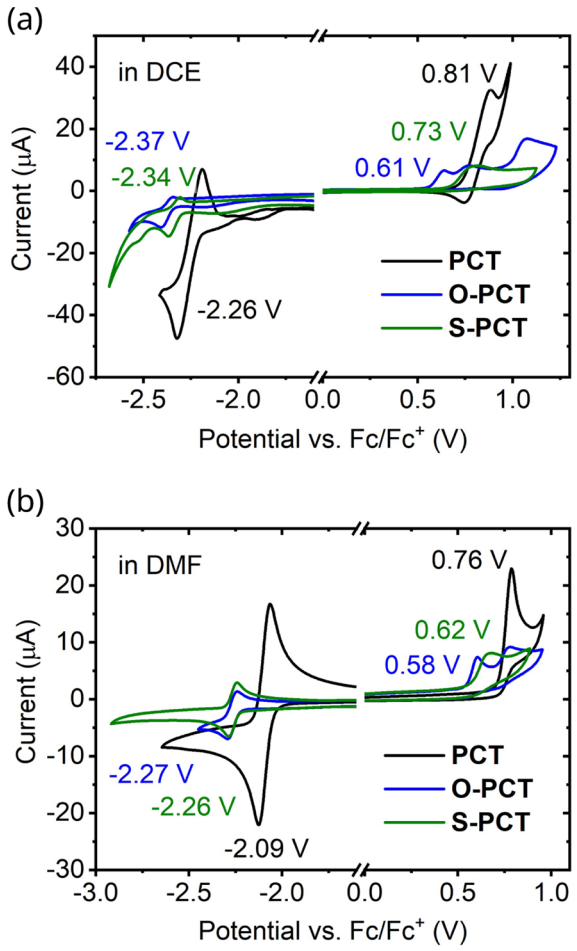

Figure 6. Cyclic voltammograms of the macrocycles in 1,2-dichloroethane (DCE) and dimethylformamide (DMF) recorded using a glassy carbon working electrode, a platinum mesh auxiliary electrode, and a silver wire quasi-reference electrode (QRE) at a scan rate of 0.1 V s^{-1}. 0.1 M tetrabutylammonium hexafluorophosphate (NBu_4PF_6) was used as the supporting electrolyte.

and on the associated local and global (anti)aromaticity of the macrocycles, the visualisation of chemical shielding tensors (VIST) method[14], which is based on the nucleus independent chemical shift[15], was used. As explained previously[6,14], VIST allows the visualisation of local variations in aromaticity and antiaromaticity in the context of the molecular structure by showing the chemical shielding tensor components using a representation of blue (shielded, aromatic) or red (deshielded, antiaromatic) dumbbells. Each tensor component relates to ring currents in a plane perpendicular to it.

The VIST plots of **O-PCT** and **S-PCT** in the neutral S_0 and T_1 states as well as in the doubly charged S_0 states are provided in Figure 7 and Figure 8, respectively. Shielding tensors were computed at the centre of the ring to probe global ring currents as well as 1 Å off the centre of the phenylene units to probe their local aromaticity. Both rotamers of the macrocycles were analysed. The corresponding VIST plots of **PCT** are

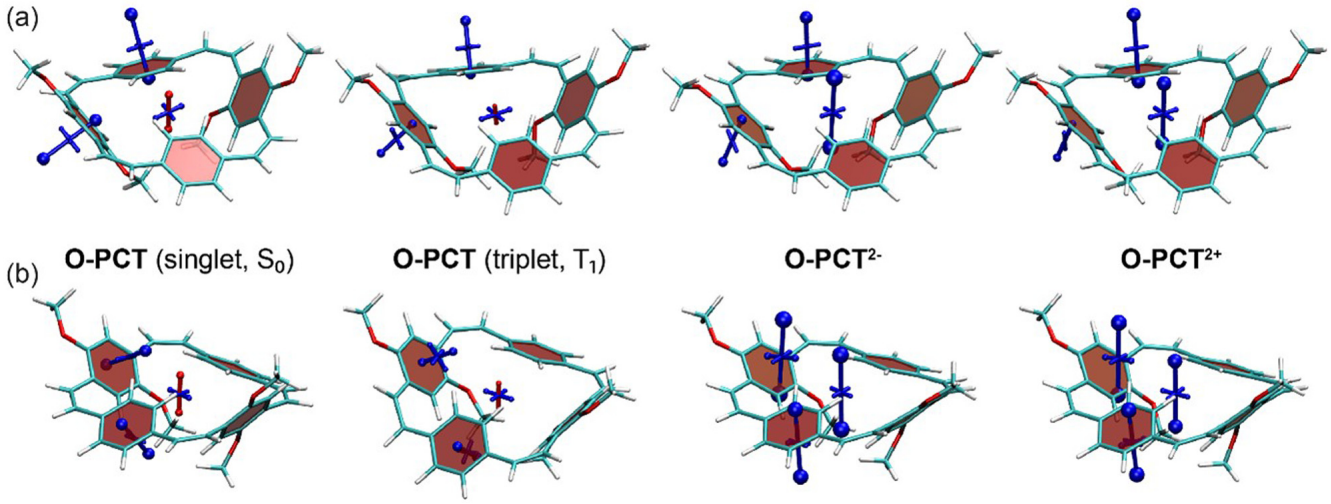

Figure 7. VIST plots for the rotamers (**a**) C_2 and (**b**) C_s of **O-PCT** (classified according to their idealised symmetry properties) in different charge and spin states. Shielded (aromatic) tensor components are shown in blue, deshielded (antiaromatic) tensor components in red. Each tensor component relates to ring currents in a plane perpendicular to it.

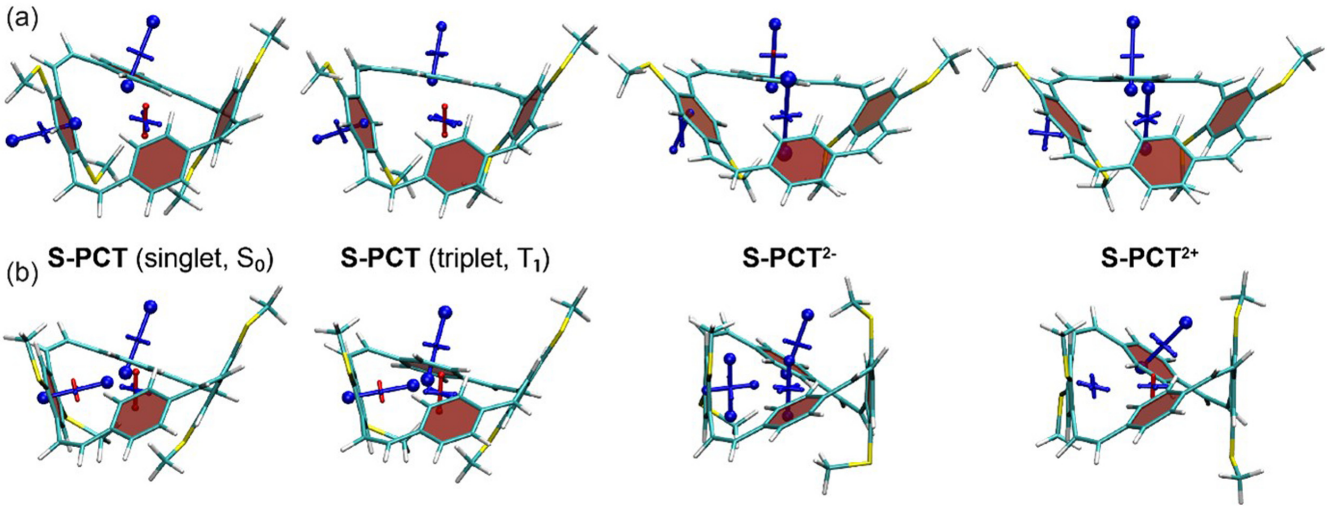

Figure 8. VIST plots for the rotamers (**a**) C_2 and (**b**) C_s of **S-PCT** (classified according to their idealised symmetry properties) in different charge and spin states. Shielded (aromatic) tensor components are shown in blue, deshielded (antiaromatic) tensor components in red. Each tensor component relates to ring currents in a plane perpendicular to it.

provided in our previous work[6]. The substituents are seen to have little effect on the magnetic properties of the neutral S_0 state. As in our previous analysis of **PCT**, the main component of the chemical shielding tensors located 1 Å off the planes of the phenylene units is shielded and almost perpendicular to the planes, indicating their local aromaticity. At the centre of the macrocycle, the tensor component perpendicular to the plane of the macrocycle is slightly deshielded, possibly indicating weak global antiaromaticity of the macrocyclic [4n] π-electron system.

In contrast to the S_0 state, the magnetic properties of the neutral T_1 state of **O-PCT** and **S-PCT** differ significantly from those of **PCT**. The VIST plots of **PCT** in the T_1 state indicate strong aromatic macrocyclic currents (and perturbed local aromaticity). This macrocyclic Baird aromaticity is obliterated by the introduction of the substituents; as the S_0 states, the neutral T_1 states of **O-PCT** and **S-PCT** are dominated by the local aromaticity of the phenylene units. To explain this phenomenon, we analysed the electronic structure in more detail by computing the natural difference orbitals (NDOs)[16] between the S_0 and T_1

states of the C_2 rotamer of **O-PCT** as an example. The NDOs, shown on the upper left in Figure 9, reveal that in the T_1 state the symmetry is broken, and the excitation is localised on one side of the molecule. More specifically, the excitation is centred around one of the vinyl groups, which is strongly twisted out of plane. Following the arguments in Ref. 17, it can be understood that Baird aromaticity would only be achieved if the transition occurred between delocalised orbitals in a cyclically conjugated structure. Next, we were interested whether similar symmetry breaking occurs for the S_1 state. Therefore, the S_1 state was optimised, and the NDOs obtained are shown on the lower left in Figure 9. In contrast to the T_1 state, the excitation in the S_1 state is evenly delocalised over the whole macrocycle. Closer inspection shows that both NDOs possess 12 nodal planes, corresponding to the quasidegenerate HOMO and LUMO of the parent [24]annulene structure. The excitation occurs between these quasidegenerate orbitals, which is the signature of excited-state aromaticity within the MO picture[17] and is, thus, consistent with the large Stokes shift observed in the measurements. The computation of shielding tensors in the S_1 state is not routinely possible. Therefore, we have computed VIST plots of the S_0 and T_1 states at the S_1 geometry instead (Figure 9, bottom right). These show enhanced antiaromaticity and aromaticity compared to the VIST plots at the geometries optimized for the respective states, further confirming that the S_1 geometry facilitates delocalisation.

Differently to the T_1 state, the VIST plots of the doubly charged states of **O-PCT** and **S-PCT** (Figure 7 and Figure 8) indicate similarly strong macrocyclic aromaticity as observed for $\mathbf{PCT^{2-}}$ and $\mathbf{PCT^{2+}}$ with the exception of the C_s rotamer of $\mathbf{S\text{-}PCT^{2+}}$ for which the VIST plot does not indicate any macrocyclic currents. In all other cases, the main component of the chemical shielding tensors at the phenylene units are tilted and almost perpendicular to the plane of the macrocycle, indicating strong perturbation of the local aromaticity by macrocyclic currents. The central shielding tensors also indicate the strong macrocyclic currents. To exemplify the change in electronic structure, we present the NDOs of the C_2 rotamer of **O-PCT** (Figure 9, upper right). The relevant attachment NDO for the dianion as well as the detachment NDO for the dication are both evenly delocalised over the entire macrocycle. More specifically, they are of similar shape as the S_1 NDOs, possessing the 12 nodal planes corresponding to the quasidegenerate [24]annulene frontier orbitals. Revisiting the C_s rotamer of $\mathbf{S\text{-}PCT^{2+}}$, we find that its relevant orbitals do not possess the required cyclically delocalised structure, thus explaining the lack of aromaticity.

A more quantitative picture is provided in Table 1 considering the shielding tensor at the centre of the ring. Specifically, we present the negative of the eigenvalue of the shielding tensor that corresponds to the dumbbell pointing out of plane in the VIST plots shown above, denoted $NICS_{ev}$. For systems of higher symmetry, $NICS_{ev}$ is equivalent to the commonly used $NICS_{zz}$ values. However, the definition used here is also applicable for the presented molecules of lower symmetry where there is no well-defined "z-axis". We present values for the original **PCT** structure, taken from Ref. 6, along with values for **O-PCT** and **S-PCT** as shown in Figure 7 and Figure 8. In addition, we present data considering the frozen structure of **PCT** optimised in the respective electronic state with added methoxy or methylthio substituents, denoted **O-PCT@PCT** and **S-PCT@PCT**. The NICS values for S_0 are all positive (between 6 and 11 ppm), indicating slight antiaromaticity along with the discussion above. Striking differences are observed for the T_1 values. These are positive and close to zero for the fully optimised structures of **O-PCT** and **S-PCT** whereas the **O-PCT@PCT** and **S-PCT@PCT** models show strong global aromaticity (-37.7 and -35.8 ppm). This highlights that Baird aromaticity is not hindered

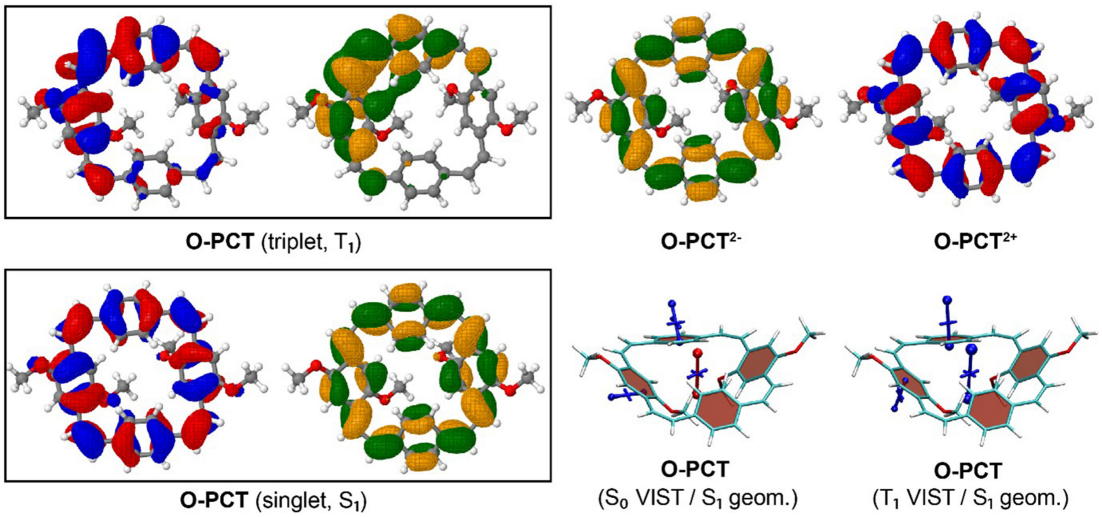

Figure 9. Dominant natural difference orbitals (NDOs) (blue/red for electron detachment; green/orange for attachment) for different electronic states of O-PCT (C_2 rotamer) and VIST plots for the S_0 and T_1 states at the S_1 geometry.

Table 1. $NICS_{ev}$ values determined at the centre of the macrocycle for the different molecules, considering always the C_2 rotamer, and electronic states.

	S_0	T_1	2^-	2^+
PCT[a]	11.0	-35.8	-38.7	-33.5
O-PCT[a]	9.6	2.8	-38.5	-29.8
S-PCT[a]	6.6	5.9	-37.2	-25.1
O-PCT@PCT[b]	7.8	-37.7	-42.5	-33.6
S-PCT@PCT[b]	8.1	-35.8	-43.0	-31.0

[a] Structure fully optimised for the respective state.

[b] Based on a frozen structure of PCT optimised for the respective state with added methoxy or methylthio substituents.

by the substituents as such but that aromaticity is lowered only when the geometry relaxes. The doubly charged states exhibit strongly negative NICS values throughout, indicating aromaticity. Finally, it is worth pointing out that the **O-PCT@PCT** shielding values for T_1, 2^-, and 2^+ are consistently higher than the corresponding values for **PCT**. This suggests that the effect of the "pure" substitution is even an enhancement in aromatic ring currents.

In summary, we find that **O-PCT** and **S-PCT** possess similar electronic structure as the parent **PCT** molecule. But similarly to our previously discussed ester-substituted molecules[6], we find that due to their lower symmetry they are further removed from the underlying idealised antiaromatic [24]annulene structure. The large Stokes shifts seen in the UV/vis absorption and PL spectra (Figure 5) are consistent with excited-state aromaticity, as seen for the optimised S_1 state of **O-PCT** in Figure 9. On the other hand, we tentatively assign the enhanced photoluminescence activity of the substituted molecules to an increased propensity for symmetry breaking, which is seen explicitly in the T_1 optimised structure and probably also plays a role for the S_1 state in terms of structural fluctuations. However, a full ab initio simulation of the resulting spectra is out of the scope of this work.

Conclusions

Our study shows that methoxy- and methylthio-substituted **PCT** derivatives can be obtained by Wittig cyclisation reactions of substituted [1,4-phenylenebis(methylene)]bis(tripheny lphosphonium) dibromides and terephthalaldehyde, in similar yields as reported for the synthesis of unsubstituted **PCT**. The required substituted Wittig cyclisation precursors can be obtained in good yields via a two/three-step procedure. Placing substituents on the terephthalaldehyde precursor did not yield the macrocycles in our attempts.

While the energy barrier for the rotation of the methoxy-substituted phenylene units in **O-PCT** was found to allow a rapid interconversion of the two rotamers, the significantly higher energy barrier for the rotation of the methylthio-substituted phenylene units in **S-PCT** resulted in distinct ^{1}H NMR signals that can be assigned to the two rotamers. Computations supported this finding, highlighting that the interconversion barrier in **S-PCT** is more than twice the barrier in **O-PCT**, increasing the expected interconversion time from 10 µs to well over one hour. The larger barrier was related to the bulkier nature of the methylthio substituents when compared to the methoxy substituents.

The introduction of the substituents was also found to alter the optoelectronic properties of **PCT**. In particular, the maximum photoluminescence (PL) intensity of **O-PCT** was found to be approximately eight times higher than for **PCT**, a feature that we tentatively assign to dynamic excited-state symmetry breaking and the associated lifting of selection rules. However, despite the increase in PL intensity, the photoluminescence quantum yield (PLQY) of the substituted macrocycles was still low. While the PL maxima were found to be redshifted, the UV-vis absorption maxima of **O-PCT** and **S-PCT** were slightly blueshifted compared to **PCT**, thus increasing the overall Stokes shifts to above 1.5 eV, which is more than three times the value of the linear **PPV** analogues. Furthermore, the electron-donating character of the substituents leads to a shift of the redox potentials to lower values, as confirmed by cyclic voltammetry measurements in two different solvents along with computations. This can be an interesting feature for tuning the properties for applications such as organic battery electrodes and further confirms the high tuneability of the properties of this compound class.

In the neutral and most of the doubly charged singlet states of **O-PCT** and **S-PCT**, the ring currents and chemical shielding do not differ significantly from those of **PCT** in the same states, according to our computational investigation using the visualisation of chemical shielding tensors (VIST) method. However, in the neutral T_1 state, the macrocyclic Baird aromaticity observed in the VIST plots of **PCT** is obliterated by the introduction of the substituents and the associated breaking of the symmetry; the molecules are dominated by the local aromaticity of the phenylene units.

In summary, the study expands the set of available [2.2.2.2]cyclophanetetraenes and offers further insights into the tuneability of the properties of this versatile compound class.

Methods

Synthetic methods

Reagents and solvents for the synthesis were purchased from commercial suppliers and used without further purification, including compounds **S-1** (Sigma-Aldrich, product number 196525), **O-2** (Sigma-Aldrilch, product number D131350), **P1** (Alfa Aesar, product number A18241.14), and **P2**

(Sigma-Aldrich, product number 808617). Purification by recycling preparative GPC was carried out on a LaboACE LC-5060 (Japan Analytical Industry Co., Tokyo, JAPAN) system equipped with a JAIGEL-2HR column and a TOYDAD800-S detector.

1,4-Bis(methylthio)benzene (S-2): Synthesis adapting a published procedure[7]. 4-Bromothioanisole (**S 1**) (508 mg, 2.5 mmol, 1.0 equiv.), CuI (119 mg, 0.63 mmol, 0.25 equiv.) and $Cu(OAc)_2$ (908 mg, 5.0 mmol, 2.0 equiv.) were added to an oven-dried vial, purged with nitrogen and sealed before adding 8 mL DMSO. The suspension was heated to 135 °C for 36 hours before cooling to room temperature (r.t.) and adding 40 mL Et_2O. The orange suspension was filtered off and washed with cold H_2O before extracting the filtrate with Et_2O (3x), drying the organic phase with Na_2SO_4 and removing the solvent under reduced pressure. Product **S-2** was purified by column chromatography using hexane/Et_2O (10:1), yielding an off-white, wax-like solid (305 mg, 1.8 mmol, 72%). ^{1}H NMR (400 MHz, $CDCl_3$): δ 7.20 (s, 4H), 2.47 (s, 6H) ppm; in accordance with the literature[7].

2,5-Bis(bromomethyl)-1,4-dimethoxybenzene (O-3): Synthesis adapting a procedure used for the bromomethylation of 1,4-dihexyloxybenzene[3]. 1,4-Dimethoxybenzene (**O-2**) (691 mg, 5.0 mmol, 1.0 equiv.) and paraformaldehyde (901 mg, 30 mmol, 6.0 equiv.) were suspended in 20 mL 1,4-dioxane. 8.0 mL HBr (30% in acetic acid) was added dropwise and the reaction was heated to 80 °C for 24 hours. The white suspension was slowly cooled to r.t., allowing the product to crystallise as a white solid. The solid was filtered off, washed twice with H_2O and recrystallised from acetonitrile (MeCN), yielding product **O-3** as white needles (837 mg, 2.6 mmol, 52%). ^{1}H NMR (400 MHz, $CDCl_3$): δ 6.87 (s, 2H), 4.54 (s, 4H), 3.87 (s, 6H) ppm; in accordance with the literature[18].

2,5-Bis(bromomethyl)-1,4-bis(methylthio)benzene (S-3): Synthesis adapting a procedure used for the bromomethylation of related substrates[3]. 1,4-Bis(methylthio)benzene (**S-2**) (375 mg, 2.2 mmol, 1.0 equiv.) and paraformaldehyde (264 mg, 8.8 mmol, 4.0 equiv.) were dissolved in 20 mL formic acid while heating to 80 °C. 3.1 mL HBr (30% in acetic acid) were added and the reaction was stirred at 80 °C for 1 hour. Paraformaldehyde (264 mg, 8.8 mmol, 4.0 equiv.) and 3.1 mL HBr (30% in acetic acid) were added three more times in intervals of 1 hour; the reaction was then stirred at 80 °C overnight using a magnetic stirrer. The white suspension was slowly cooled to r.t., allowing the product to crystallise as an off-white solid. Product **S-3** was isolated by filtering and washing with MeOH (685 mg, 1.9 mmol, 87%). ^{1}H NMR (400 MHz, CD_2Cl_2): δ 7.28 (s, 2H), 4.63 (s, 4H), 2.52 (s, 6H) ppm. ^{1}H NMR (400 MHz, $CDCl_3$): δ 7.26 (s, 2H, overlaps with solvent peak), 4.61 (s, 4H), 2.52 (s, 6H) ppm; ^{13}C{^{1}H} NMR (101 MHz, $CDCl_3$): δ 137.2, 136.0, 129.5, 31.1, 16.7 ppm. HRMS (*m/z*): $[M]^+$ calcd for $C_{10}H_{12}S_2Br_2$: 353.8742, found: 353.8733 (APCI).

[(2,5-dimethoxy-1,4-phenylene)bis(methylene)]bis (triphenylphosphonium) dibromide (O-P1): Substrate **O-3** (713 mg, 2.2 mmol, 1.0 equiv.) and PPh_3 (2.02 g, 7.7 mmol, 3.5 equiv.) were suspended in 7.5 mL anhydrous toluene in a sealed vial under nitrogen and heated to 120 °C overnight. The white precipitate was filtered and washed with toluene and Et_2O. Product **O-P1** was isolated as a white solid (1.56 g, 1.8 mmol, 84%). ^{1}H NMR (400 MHz, $CDCl_3$): δ 7.79 – 7.73 (m, 6H), 7.73 – 7.61 (m, 24H), 6.96 (d, *J* = 1.9 Hz, 2H), 5.23 (d, *J* = 12.8 Hz, 4H), 2.97 (s, 6H) ppm. ^{31}P{^{1}H} NMR (162 MHz, $CDCl_3$): δ 21.82 ppm. HRMS (*m/z*): $[M–2Br]^{2+}$ calcd for $C_{46}H_{42}Br_2O_2P_2$: 344.1330, found: 344.1325 (ESI).

[(2,5-bis(methylthio)-1,4-phenylene)bis(methylene)] bis(triphenylphosphonium) dibromide (S-P1): Substrate **S-3** (605 mg, 1.7 mmol, 1.0 equiv.) and PPh_3 (1.34 g, 5.1 mmol, 3.0 equiv.) were suspended in 25 mL anhydrous toluene in a sealed vial under nitrogen and heated to 120 °C overnight. The white precipitate was filtered and washed with toluene and Et_2O. Product **S-P1** was isolated as a white solid (1.30 g, 1.5 mmol, 87%) after triturating in boiling *n*-butanol for 1.5 h for further purification. ^{1}H NMR (400 MHz, $CDCl_3$): δ 7.82 – 7.74 (m, 6H), 7.73 – 7.59 (m, 24H), 7.13 (d, *J* = 2.1 Hz, 2H), 5.52 (d, *J* = 12.5 Hz, 4H), 1.71 (s, 6H) ppm. ^{31}P{^{1}H} NMR (162 MHz, $CDCl_3$): δ 22.00 ppm. HRMS (*m/z*): $[M–2Br]^{2+}$ calcd for $C_{46}H_{42}Br_2P_2S_2$: 360.1101, found: 360.1111 (ESI).

2,5-Dibromoterephthalaldehyde (Br-P2): Synthesis adapting a published procedure[8]. Terephthalaldehyde (**P2**) (8.05 g, 60 mmol, 1.0 equiv.) was dissolved in 80 mL conc. H_2SO_4 at 60 °C. N-Bromosuccinimide (NBS) (23.5 g, 132 mmol, 2.2 equiv.) was added in small portions over 30 min. The reaction was then stirred for 3 hours at 60 °C before cooling to r.t. and pouring onto ice. The white precipitate was washed with aq. $NaHCO_3$ and brine before being recrystallised from $CHCl_3$. **Br-P2** was isolated as off-white crystals (9.30 g, 31.9 mmol, 53%). ^{1}H NMR (400 MHz, $CDCl_3$): δ 10.35 (s, 2H), 8.16 (s, 2H) ppm; in accordance with the literature[19].

2,5-Bis(methylthio)terephthalaldehyde (S-P2): Synthesis adapting a published procedure[9]. **Br-P2** (992 mg, 3.4 mmol, 1.0 equiv.) was dissolved in 70 mL DMF before adding $NaSCH_3$ (498 mg, 7.1 mmol, 2.1 equiv.) at r.t. The dark red solution was stirred for 10 minutes and then poured into 250 mL 1M HCl, forming an orange precipitate. The mixture was extracted with $CHCl_3$ (3x), the organic phase dried with Na_2SO_4 and the solvent removed under reduced pressure. The crude product was recrystallised from MeCN, yielding **S-P2** as an orange solid (630 mg, 2.8 mmol, 82%). ^{1}H NMR (400 MHz, $CDCl_3$): δ 10.41 (s, 2H), 7.80 (s, 2H), 2.57 (s, 6H) ppm; in accordance with the literature[9].

Methoxy-substituted [2.2.2.2]paracyclophanetetraene O-PCT: Wittig cyclisation precursor **O-P1** (1.19 g, 1.4 mmol, 1.0 equiv.) and terephthalaldehyde (**P2**) (188 mg, 1.4 mmol, 1.0 equiv.) were dissolved in 70 mL anhydrous DMF under nitrogen, purged with nitrogen for 5 min and cooled to -40 °C using an MeCN/dry ice bath. Lithium methoxide (159 mg, 4.2 mmol, 3.0 equiv.) was dissolved in 18 mL anhydrous MeOH by sonication, purged with nitrogen for 2 minutes (purge carefully

to avoid precipitation) and added to the reaction over 9 hours using a syringe pump. The rate of addition was adjusted to maintain a faint red colour of the solution. After complete addition of the base, the reaction was stirred overnight, using a magnetic stirrer, while warming to r.t. The resulting suspension was poured into H_2O and extracted with Et_2O (3x), the organic phase dried with Na_2SO_4 and the solvent removed in vacuo. The obtained solid was dissolved CH_2Cl_2 and flashed over silica using CH_2Cl_2 as the eluent until the solvent ran clear (to remove the Wittig reaction side product triphenylphosphine oxide (TPPO)). The crude product was purified by recycling preparative GPC using $CHCl_3$ as the eluent, yielding **O-PCT** as a yellow oil that crystallised slowly over time (32 mg, 0.06 mmol, 9%). ^{1}H NMR (400 MHz, $CDCl_3$): δ 7.08 (s, 8H), 6.72 (s, 4H), 6.58 (d, *J* = 12.2 Hz, 4H), 6.52 (d, *J* = 12.1 Hz, 4H), 3.55 (s, 12H) ppm. ^{13}C{^{1}H} NMR (101 MHz, $CDCl_3$): δ 151.1, 136.0, 130.8, 128.8, 127.0, 126.2, 113.4, 56.3 ppm. HRMS (*m/z*): $[M]^+$ calcd for $C_{36}H_{32}O_4$: 528.2301, found: 528.2301 (ESI).

Methylthio-substituted [2.2.2.2]paracyclophanetetraene S-PCT: Wittig cyclisation precursor **S-P1** (1.00 g, 1.14 mmol, 1.0 equiv.) and terephthalaldehyde (**P2**) (153 mg, 1.14 mmol, 1.0 equiv.) were dissolved in 35 mL anhydrous DMF under nitrogen, purged with nitrogen for 5 min and cooled to -40 °C using an MeCN/dry ice bath. Lithium methoxide (130 mg, 3.4 mmol, 3.0 equiv.) was dissolved in 9 mL anhydrous MeOH by sonication, purged with nitrogen for 2 minutes (purge carefully to avoid precipitation) and added to the reaction over 9 hours using a syringe pump. The rate of addition was adjusted to maintain a faint red colour of the solution. After complete addition of the base, the reaction was stirred overnight while warming to r.t. The resulting suspension was poured into H_2O and extracted with Et_2O (3x), the organic phase dried with Na_2SO_4 and the solvent removed in vacuo. The obtained solid was dissolved CH_2Cl_2 and flashed over silica using CH_2Cl_2 as the eluent until the solvent ran clear (to remove the Wittig reaction side product triphenylphosphine oxide (TPPO)). The crude product was purified by recycling preparative GPC using $CHCl_3$ as the eluent, yielding **S-PCT** as an orange solid (48 mg, 0.08 mmol, 14%). ^{1}H NMR measurements (including measurements at elevated temperature) suggest that the product is a mixture of two rotamers (ratio approx. 10:1, determined from ^{1}H NMR integrals). *Main rotamer:* ^{1}H NMR (400 MHz, $CDCl_3$): δ 6.97 (s, 4H), 6.95 (s, 8H), 6.63 (d, *J* = 12.0 Hz, 4H), 6.57 (d, *J* = 12.0 Hz, 4H), 2.14 (s, 12H) ppm. ^{13}C{^{1}H} NMR (101 MHz, $CDCl_3$): δ 137.0, 135.6, 134.2, 131.5, 129.0, 128.2, 127.0, 16.0 ppm. ^{1}H NMR (400 MHz, $CDCl_3$, 50 °C): δ 7.00 (s, 4H), 6.95 (s, 8H), 6.65 (d, *J* = 11.9 Hz, 4H), 6.58 (d, *J* = 11.9 Hz, 4H), 2.14 (s, 12H) ppm. *Minor rotamer:* ^{1}H NMR (400 MHz, $CDCl_3$): 7.00 (s, 4H), 6.98 (s, 8H), 6.58 (s, 8H), 2.22 (s, 12H) ppm. ^{1}H NMR (400 MHz, $CDCl_3$, 50 °C): δ 7.03 (s, 4H), 6.99 (s, 8H), 6.58 (s, 8H), 2.21 (s, 12H) ppm. HRMS (*m/z*): $[M+H]^+$ calcd for $C_{36}H_{32}S_4$: 593.1460, found: 593.1444 (APCI).

Measurement methods and instrumentation

NMR spectra were recorded in $CDCl_3$ solution at 400 MHz for ^{1}H, 101 MHz for ^{13}C, and 162 MHz for ^{31}P on a Bruker AV-400 spectrometer. High-resolution mass spectrometry (HRMS) was carried out on systems from Thermo Scientific (Thermo Scientific Q-Exactive/Dionex Ultimate 3000) for atmospheric pressure chemical ionization (APCI) and Waters (Waters LCT Premier (ES-ToF)/Acquity i-Class) for electrospray ionization (ESI). While the Thermo Scientific system gives the actual mass of the ionized compounds, the Waters system is calibrated to give the mass of the neutral compounds. This was considered when calculating the *m/z* values for comparison with the measurements.

UV-vis absorption spectra were recorded on an Agilent Cary 60 UV-vis spectrophotometer at room temperature. The measurements of the macrocycles were carried out with 5 μM solutions in $CHCl_3$ at a scan rate of 300 nm min^{-1} and a data interval of 0.5 nm. The baseline was corrected for plotting the data in Figure 5. Photoluminescence (PL) spectra of the macrocycles were acquired on an Agilent Cary Eclipse fluorescence spectrophotometer with 5 μM solutions in $CHCl_3$ at a scan rate of 120 nm min^{-1} and a data interval of 1 nm. The excitation and emission slits were set to 5 nm, the emission and excitation filters were set to 'auto' setting, and the detector voltage was set to 'high' (800 V). To facilitate a comparison, these are the same settings as used in our previous work on a set of ester-substituted macrocycles[6]. For the relative determination of the photoluminescence quantum yield (PLQY) of the macrocycles, UV-vis absorption and PL spectra of a 50 μM solution of quinine in 0.05 M H_2SO_4 were recorded as a reference. For the PL measurements of this reference, a neutral density filter (ND 1.5) was used in the emission pathway to enable measurements under the same instrument settings as used for the macrocycles. The use of neutral density filters is recommended to enable the determination of very small quantum yields (<1%) relative to a moderately to highly emissive reference.[20] For the calculation of the PLQYs of the macrocycles according Ref. 20, a PLQY of 60% was assumed for the reference[21].

Cyclic voltammetry (CV) measurements were carried out at arbitrary concentration using a glassy carbon working electrode, a platinum mesh auxiliary electrode, and a silver wire quasi-reference electrode (QRE) at a scan rate of 0.1 V s^{-1}. 0.1 M Tetrabutylammonium hexafluorophosphate (NBu_4PF_6) in dichloroethane (DCE) or dimethylformamide (DMF) were used as the supporting electrolyte solution. Ferrocene (Fc) was measured as reference. The solutions were purged with nitrogen for 5 min prior to the measurements. However, the presences of a reduction process at around -1.4 V vs. Fc/Fc$^+$ in the measurements suggests that some residual oxygen was not efficiently removed by the purging process[22]. This reduction process was also present when measuring the supporting electrolyte solutions only (without a sample), corroborating that the process does not involve the macrocycles. In line with best practice, the redox potentials were estimated from the half-wave potential ($E^{1/2}$) when reversibility was observed and from the inflection-point potential (E^i) when no reversibility was observed[23].

Computational methods

Geometries for the neutral S_0 and T_1 states as well as the dianion and dication were optimized in vacuum using density

functional theory (DFT) with the PBE0 functional[24,25] along with the def2-SV(P) basis set[26] and the D3 dispersion correction[27] in its optimised power version[28]. Transition state (TS) energies were optimized via a constrained optimization, fixing two of the phenylene-vinylene torsion angles, considering that a full TS optimization did not converge for **S-PCT** and verifying that the energies between this method and the full optimization were consistent for **O-PCT**. Interconversion times (t) between rotamers were estimated via the Eyring equation

$$\frac{1}{t} = \frac{kT}{h} \exp\left(-\frac{\Delta_a E}{kT}\right)$$

where k and h are the Boltzmann and Planck constants, T = 298 K is the temperature and $\Delta_a E$ is the computed activation barrier. Redox potentials were computed using the PBE0 functional along with the def2-SVPD basis set using a conductor-like polarizable continuum model[29] considering a dielectric constant of 10.125 to represent 1,2-dichloroethane (DCE) and following the procedure described in detail in Ref. 6. All these computations were carried out in Q-Chem 5.3[30,31]. S_1 states were optimised using time-dependent (TD) DFT with the ωPBEh functional[32] (using ω=0.1 a.u. and 20% global Hartree-Fock exchange) along with the def2-SV(P) basis set and the D3 dispersion correction using the same D3-parameters as for PBE0.

Chemical shielding tensors were computed at the PBE0/def2-SVP level using gauge including atomic orbitals[33] as implemented in Gaussian 09[34]. Shielding tensors were represented graphically using the VIST (visualisation of chemical shielding tensors) method[14] as implemented in TheoDORE 2.4[35] using cclib[36] for some of the file parsing work and VMD[37] for the final graphical representation. Shielding tensors for the **O/S-PCT@PCT** structures were computed using the optimised structure of **PCT** for the respective state, freezing this structure, adding methoxy/methylthio substituents, and optimising only the geometry of those groups.

NDOs[16] for the T_1 and charged states were computed using TheoDORE following two independent DFT calculations. NDOs for the S_1 state were computed directly within Q-Chem after the TDDFT computation.

Data availability

Underlying data

Zenodo: Research data for "[2.2.2.2]Paracyclophanetetraenes (PCTs): cyclic structural analogues of poly(p-phenylene vinylene)s (PPVs)". https://doi.org/10.5281/zenodo.6323475[38]

This project contains the following data:

- The underlying experimental research data (^{1}H NMR, ^{13}C NMR, ^{31}P NMR, high-resolution mass spectrometry (HRMS), UV-vis absorption, photoluminescence (PL), cyclic voltammetry)
- The underlying computational research data (molecular geometries, input/output files for Q-Chem, Gaussian, and TheoDORE)

The ^{1}H NMR, ^{13}C NMR, and ^{31}P NMR spectra are also available via ChemSpider. See CSIDs: 120300 (**S-2**), 3332510 (**O-3**), 110417237 (**S-3**), 110417244 (**O-P1**), 110417245 (**S-P1**), 14757439 (**Br-P2**), 110417240 (**S-P2**), 110417241 (**O-PCT**), and 110417242 (**S-PCT**).

Acknowledgements

We thank Ugurcan Sal for contributing to synthetic experiments, Lisa Haigh for HRMS measurements, and Peter Haycock for NMR measurements at elevated temperature (all Imperial College London).

References

1. Blayney AJ, Perepichka IF, Wudl F, *et al.*: **Advances and Challenges in the Synthesis of Poly(*p*-phenylene vinylene)-Based Polymers.** *Isr J Chem.* 2014; **54**(5–6): 674–688.
Publisher Full Text
2. Schönbein AK, Wagner M, Blom PWM, *et al.*: **Quantifying the Kinetics of the Gilch Polymerization toward Alkoxy-Substituted Poly(*p*-phenylene vinylene).** *Macromolecules.* 2017; **50**(13): 4952–4961.
Publisher Full Text
3. Rimmele M, Ableidinger K, Marsh AV, *et al.*: **Thioalkyl- and sulfone-substituted poly(*p*-phenylene vinylene)s.** *Polym Chem.* 2019; **10**(6): 738–750.
Publisher Full Text
4. Thulin B, Wennerström O, Högberg HE: **Simple Synthesis of [2.2.2.2]-Paracyclophane-1,9,17,25-Tetraene by a Wittig Reaction.** *Acta Chem Scand Ser B.* 1975; **29**(1): 138–139.
Publisher Full Text
5. Eder S, Yoo DJ, Nogala W, *et al.*: **Switching between Local and Global Aromaticity in a Conjugated Macrocycle for High-Performance Organic Sodium-Ion Battery Anodes.** *Angew Chem Int Ed.* 2020; **59**(31): 12958–12964.
PubMed Abstract | Publisher Full Text | Free Full Text
6. Rimmele M, Nogala W, Seif-Eddine M, *et al.*: **Functional group introduction and aromatic unit variation in a set of π-conjugated macrocycles: revealing the central role of local and global aromaticity.** *Org Chem Front.* 2021; **8**(17): 4730–4745.
PubMed Abstract | Publisher Full Text | Free Full Text
7. Amal Joseph PJ, Priyadarshini S, Kantam ML, *et al.*: **Investigation of the scope and mechanism of copper catalyzed regioselective methylthiolation of aryl halides.** *Tetrahedron.* 2013; **69**(38): 8276–8283.
Publisher Full Text
8. Prusinowska N, Bardziński M, Janiak A, *et al.*: **Sterically Crowded Trianglimines-Synthesis, Structure, Solid-State Self-Assembly, and Unexpected Chiroptical Properties.** *Chem Asian J.* 2018; **13**(18): 2691–2699.
PubMed Abstract | Publisher Full Text
9. Yamamoto T, Nishimura T, Mori T, *et al.*: **Largely π-Extended Thienoacenes with Internal Thieno[3,2-*b*]thiophene Substructures: Synthesis, Characterization, and Organic Field-Effect Transistor Applications.** *Org Lett.* 2012; **14**(18): 4914–4917.
PubMed Abstract | Publisher Full Text
10. Szakács Z, Glöcklhofer F, Plasser F, *et al.*: **Excited-state symmetry breaking in**

9,10-dicyanoanthracene-based quadrupolar molecules: the effect of donor-acceptor branch length. *Phys Chem Chem Phys.* 2021; **23**(28): 15150–15158.
PubMed Abstract | Publisher Full Text | Free Full Text

11. Gierschner J, Mack HG, Lüer L, *et al.*: **Fluorescence and absorption spectra of oligophenylenevinylenes: Vibronic coupling, band shapes, and solvatochromism.** *J Chem Phys.* 2002; **116**(19): 8596–8609.
Publisher Full Text

12. Su WF, Yeh KM, Chen Y: **Synthesis and optoelectronic properties of luminescent poly(*p*-phenylenevinylene) derivatives containing electron-transporting 1,3,4-oxadiazole groups.** *J Polym Sci Part A Polym Chem.* 2007; **45**(18): 4377–4388.
Publisher Full Text

13. Kotani R, Liu L, Kumar P, *et al.*: **Controlling the S_1 Energy Profile by Tuning Excited-State Aromaticity.** *J Am Chem Soc.* 2020; **142**(35): 14985–14992.
PubMed Abstract | Publisher Full Text

14. Plasser F, Glöcklhofer F: **Visualisation of Chemical Shielding Tensors (VIST) to Elucidate Aromaticity and Antiaromaticity.** *Eur J Org Chem.* 2021; **2021**(17): 2529–2539.
PubMed Abstract | Publisher Full Text | Free Full Text

15. Chen Z, Wannere CS, Corminboeuf C, *et al.*: **Nucleus-Independent Chemical Shifts (NICS) as an Aromaticity Criterion.** *Chem Rev.* 2005; **105**(10): 3842–3888.
PubMed Abstract | Publisher Full Text

16. Plasser F, Wormit M, Dreuw A: **New tools for the systematic analysis and visualization of electronic excitations. I. Formalism.** *J Chem Phys.* 2014; **141**(2): 024106.
PubMed Abstract | Publisher Full Text

17. Plasser F: **Exploitation of Baird Aromaticity and Clar's Rule for Tuning the Triplet Energies of Polycyclic Aromatic Hydrocarbons.** *Chemistry.* 2021; **3**(2): 532–549.
Publisher Full Text

18. Kotha S, Cheekatla SR, Lal S, *et al.*: **Pentacycloundecane (PCUD)-Based Cage Frameworks as Potential Energetic Materials: Syntheses and Characterization.** *Asian J Org Chem.* 2020; **9**(12): 2116–2126.
Publisher Full Text

19. Meindl B, Pfennigbauer K, Stöger B, *et al.*: **Double Ring-Closing Approach for the Synthesis of 2,3,6,7-Substituted Anthracene Derivatives.** *J Org Chem.* 2020; **85**(12): 8240–8244.
PubMed Abstract | Publisher Full Text

20. Würth C, Grabolle M, Pauli J: **Relative and absolute determination of fluorescence quantum yields of transparent samples.** *Nat Protoc.* 2013; **8**(8): 1535–1550.
PubMed Abstract | Publisher Full Text

21. Brouwer AM: **Standards for photoluminescence quantum yield measurements in solution (IUPAC Technical Report).** *Pure Appl Chem.* 2011; **83**(12): 2213–2228.
Publisher Full Text

22. Elgrishi N, Rountree KJ, McCarthy BD, *et al.*: **A Practical Beginner's Guide to Cyclic Voltammetry.** *J Chem Educ.* 2018; **95**(2): 197–206.
Publisher Full Text

23. Espinoza EM, Clark JA, Soliman J, *et al.*: **Practical Aspects of Cyclic Voltammetry: How to Estimate Reduction Potentials When Irreversibility Prevails.** *J Electrochem Soc.* 2019; **166**(5): H3175–H3187.
Publisher Full Text

24. Perdew JP, Burke K, Ernzerhof M: **Generalized Gradient Approximation Made Simple.** *Phys Rev Lett.* 1996; **77**(18): 3865–3868.
PubMed Abstract | Publisher Full Text

25. Adamo C, Barone V: **Toward reliable density functional methods without adjustable parameters: The PBE0 model.** *J Chem Phys.* 1999; **110**(13): 6158–6170.
Publisher Full Text

26. Weigend F, Ahlrichs R: **Balanced basis sets of split valence, triple zeta valence and quadruple zeta valence quality for H to Rn: Design and assessment of accuracy.** *Phys Chem Chem Phys.* 2005; **7**(18): 3297–3305.
PubMed Abstract | Publisher Full Text

27. Grimme S, Antony J, Ehrlich S, *et al.*: **A consistent and accurate *ab initio* parametrization of density functional dispersion correction (DFT-D) for the 94 elements H-Pu.** *J Chem Phys.* 2010; **132**(15): 154104.
PubMed Abstract | Publisher Full Text

28. Witte J, Mardirossian N, Neaton JB, *et al.*: **Assessing DFT-D3 Damping Functions Across Widely Used Density Functionals: Can We Do Better?** *J Chem Theory Comput.* 2017; **13**(5): 2043–2052.
PubMed Abstract | Publisher Full Text

29. Barone V, Cossi M: **Quantum Calculation of Molecular Energies and Energy Gradients in Solution by a Conductor Solvent Model.** *J Phys Chem A.* 1998; **102**(11): 1995–2001.
Publisher Full Text

30. Shao Y, Gan Z, Epifanovsky E, *et al.*: **Advances in molecular quantum chemistry contained in the Q-Chem 4 program package.** *Mol Phys.* 2015; **113**(2): 184–215.
Publisher Full Text

31. Krylov AI, Gill PMW: **Q-Chem: an engine for innovation.** *Wiley Interdiscip Rev Comput Mol Sci.* 2013; **3**(3): 317–326.
Publisher Full Text

32. Rohrdanz MA, Martins KM, Herbert JM: **A long-range-corrected density functional that performs well for both ground-state properties and time-dependent density functional theory excitation energies, including charge-transfer excited states.** *J Chem Phys.* 2009; **130**(5): 054112.
PubMed Abstract | Publisher Full Text

33. Cheeseman JR, Trucks GW, Keith TA, *et al.*: **A comparison of models for calculating nuclear magnetic resonance shielding tensors.** *J Chem Phys.* 1996; **104**(14): 5497–5509.
Publisher Full Text

34. Frisch MJ, Trucks GW, Schlegel HB, *et al.*: **Gaussian 09, Revision E.01.** Wallingford, CT, 2013.

35. Plasser F: **TheoDORE: A toolbox for a detailed and automated analysis of electronic excited state computations.** *J Chem Phys.* 2020; **152**(8): 084108.
PubMed Abstract | Publisher Full Text

36. O'boyle NM, Tenderholt AL, Langner KM: **cclib: A library for package-independent computational chemistry algorithms.** *J Comput Chem.* 2008; **29**(5): 839–845.
PubMed Abstract | Publisher Full Text

37. Humphrey W, Dalke A, Schulten K: **VMD: visual molecular dynamics.** *J Mol Graph.* 1996; **14**(1): 33–38, 27–8.
PubMed Abstract | Publisher Full Text

38. Pletzer M, Plasser F, Rimmele M, *et al.*: **Research data for "[2.2.2.2]Paracyclophanetetraenes (PCTs): cyclic structural analogues of poly(p-phenylene vinylene)s (PPVs)".** [Data set]. *Zenodo.* 2021.
http://www.doi.org/10.5281/zenodo.6323475

Open Peer Review

Current Peer Review Status: ✔ ✔

Version 2

Reviewer Report 05 April 2022

https://doi.org/10.21956/openreseurope.15764.r28785

✔ **Miłosz Pawlicki**
Department of Chemistry, Jagiellonian University, Kraków, Poland

The revised manuscript of Glöcklhofer and co-workers addresses all crucial points gathered in both previous reports and currently can be accepted without reservations. I highly appreciate the presented discussion on the fluorescence quantum yields and extended presentation of the magnetic properties. As mentioned in my previous report it is important to compare the descriptors of diatropic/paratropic behaviour what directs us to more comprehensive picture of aromaticity/antiaromaticity and the properties of those systems.

Competing Interests: No competing interests were disclosed.

Reviewer Expertise: Organic synthesis, pi-conjugation, aromaticty, spectroscopy,

I confirm that I have read this submission and believe that I have an appropriate level of expertise to confirm that it is of an acceptable scientific standard.

Version 1

Reviewer Report 14 February 2022

https://doi.org/10.21956/openreseurope.14798.r28154

? **Miłosz Pawlicki**
Department of Chemistry, Jagiellonian University, Kraków, Poland

The presented material shows a specific construction of cyclic motifs incorporating p-phenylenes substituted with heteroatoms - oxygen or sulfur. All the conclusions are focusing on the observed changes in conjugation triggered by the excitation but are also theoretically analysed for redox modified structures.
The dynamic process recorded within the skeleton (Fig .4) can have a significant influence on the emission efficiency. I would recommend an extension of the scope of experiments with a viscosity dependent measurements and checking is there any influence of the dynamic behaviour on the final fluorescence outcome. The dynamic of the excited state (S1) is very sensitive to several factors including a change of aromatic character mentioned by the Authors but it also indicates the stability of the excited state in addition to adding another proof for the observed behaviour. I would suggest extending the discussion by this data that will be beneficial for a deeper understanding of observed properties. The second crucial parameter for fluorescence observed within any molecule is a quantum yield which has not been included in the presented material. Extension of the analysis on those two key parameters for all reported systems will create a comprehensive picture of the conjugation observed in those structural motifs.
The presented material discusses two different isomers that differed by the rotation of disubstituted phenylene but can the described dynamic process be treated as a simple rotation? While looking at the proximity of present substituents it potentially can be analysed as a concerted process where a move of one substituted phenylenes will cause a deep change in the whole system forcing also the move of unsubstituted phenylenes. I would recommend an extension of this discussion by incorporation of additional data explaining the isomerisation which will bring the Reader a set of conformational changes necessary for observing switching from one isomer to another.
The theoretical analysis of changes in delocalisation relies on the VIST analysis - an original approach for visuliation of the changes in aromatic/antiaromatic character developed by the Authors of this manuscript. I would suggest to compare the observed behaviour with any other theoretical descriptors of aromaticity/antiaromaticity (e.g. NICS(0,1,2)) which will eventually bring a comprehensive picture.
In conclusion, the presented material brings insight to macrocyclic systems constructed with p-phenylenes showing modulation of conjugation within those systems potentially beneficial for several fields.

Is the work clearly and accurately presented and does it cite the current literature?
Yes

Is the study design appropriate and does the work have academic merit?
Yes

Are sufficient details of methods and analysis provided to allow replication by others?
Yes

If applicable, is the statistical analysis and its interpretation appropriate?
Not applicable

Are all the source data underlying the results available to ensure full reproducibility?
Yes

Are the conclusions drawn adequately supported by the results?

Partly

Competing Interests: No competing interests were disclosed.

Reviewer Expertise: Organic synthesis, pi-conjugation, aromaticty, spectroscopy,

I confirm that I have read this submission and believe that I have an appropriate level of expertise to confirm that it is of an acceptable scientific standard, however I have significant reservations, as outlined above.

Author Response 03 Mar 2022

Florian Glöcklhofer, Imperial College London, London, UK

Thank you for reviewing and approving our article with reservations. We would like to respond to the comments below and hope that with the changes made in response the article can be approved for indexing in bibliographic databases. (Reviewer comments in italics)

The dynamic process recorded within the skeleton (Fig .4) can have a significant influence on the emission efficiency. I would recommend an extension of the scope of experiments with a viscosity dependent measurements and checking is there any influence of the dynamic behaviour on the final fluorescence outcome. The dynamic of the excited state (S1) is very sensitive to several factors including a change of aromatic character mentioned by the Authors but it also indicates the stability of the excited state in addition to adding another proof for the observed behaviour. I would suggest extending the discussion by this data that will be beneficial for a deeper understanding of observed properties. The second crucial parameter for fluorescence observed within any molecule is a quantum yield which has not been included in the presented material. Extension of the analysis on those two key parameters for all reported systems will create a comprehensive picture of the conjugation observed in those structural motifs.
Response: We thank the reviewer for these recommendations. We have now determined the PLQYs of the macrocycles using quinine in 0.05 M H_2SO_4 as the reference to further support the conclusions of the article. Despite the observed increase in PL intensity upon introduction of the substituents, all three investigated macrocycles are weak emitters; PLQYs of 0.06% for **PCT**, 0.65% for **O-PCT**, and 0.56% for **S-PCT** were determined. Due to the large difference in PLQY between the reference and the macrocycles, neutral density filters had to be used to enable PL measurements of the reference under the same instrument settings as used for the macrocycles. We believe this relative determination of the PLQYs can provide a good indication of the order of magnitude, but we suggest refraining from an overinterpretation of the exact values due to the potential sources of error in the determination. We have added the following sentence in the results and discussion section of the article and updated the conclusions and methods sections as well as the provided underlying research data accordingly: “Despite the increase in PL intensity upon introduction of the substituents, all three macrocycles are still weak emitters, with a relative determination of the photoluminescence quantum yield (PLQY) indicating values of <1% for **O-PCT** and **S-PCT** and <0.1% for **PCT**.” We agree that viscosity dependent measurements could provide even further insights and conclusions. Nevertheless, we believe that the current conclusions of the article are adequately supported by the provided results and that

further photophysical measurements are beyond the scope of this article. The article does not intend to provide a detailed photophysical study of the synthesised macrocycles but, in addition to the synthesis and computational analysis of the macrocycles, aims to provide some basic photophysical and electrochemical characterisation as well as a comparison of the characterisation results obtained for the different macrocycles. From the careful language used in the discussion of the photoluminescence intensities ("tentatively assigned to symmetry breaking in the excited state", "the spectra suggest that symmetry breaking is only a dynamic effect") and in the conclusions ("a feature that we assign to dynamic excited-state symmetry breaking"), we believe it should be clear that further photophysical studies are required for a better understanding of the effects and a more definitive explanation. We have added "tentatively" in the conclusions to further clarify this there.

The presented material discusses two different isomers that differed by the rotation of disubstituted phenylene but can the described dynamic process be treated as a simple rotation? While looking at the proximity of present substituents it potentially can be analysed as a concerted process where a move of one substituted phenylenes will cause a deep change in the whole system forcing also the move of unsubstituted phenylenes. I would recommend an extension of this discussion by incorporation of additional data explaining the isomerisation which will bring the Reader a set of conformational changes necessary for observing switching from one isomer to another.
Response: We agree with the reviewer that the switch between the two isomers is a non-trivial dynamical process. Indeed, it was challenging to find a well-defined reaction coordinate for this process. The purpose of the computations performed was to illustrate the qualitative difference between the reaction barriers to explain the NMR signals. A full mechanistic study of the interconversion process is out of the scope of this study.

The theoretical analysis of changes in delocalisation relies on the VIST analysis - an original approach for visuliation of the changes in aromatic/antiaromatic character developed by the Authors of this manuscript. I would suggest to compare the observed behaviour with any other theoretical descriptors of aromaticity/antiaromaticity (e.g. NICS(0,1,2)) which will eventually bring a comprehensive picture.
Response: Following the reviewer's suggestion, we have added NICS values in the paper, see Table 1. Indeed the NICS value printed is directly related to the size of the dumbbell in the VIST plot.

Competing Interests: No competing interests were disclosed.

Reviewer Report 23 December 2021

https://doi.org/10.21956/openreseurope.14798.r28148

Weixuan Zeng
Department of Chemistry, University of Cambridge, Cambridge, UK

The manuscript by Pletzer and co-workers described a combined experimental and computational study on the methoxy- and methylthio-substituented [2.2.2.2]paracyclophanetetraene (PCT). The rotamers cased by the substituents not only changed the geometries but also the symmetry properties of the compounds, which resulted in significant changes in their excited-state aromaticity features. The reviewer thought this work well extended the previous study on the 'PCT' series by the authors and got some interesting results for readers, and therefore reaches the acceptable standard as this form.

Here're some recommendations for further improvement:

1. More accurate concentration of the solution samples for the UV-Vis and PL measurements is recommended to be provided. Further discussion on their photoluminescent quantum yields instead of the comparison of the intensity would be more suitable for the discussion about the photophysics characters of the compounds.

2. The chemical shift features as aromaticity criteria might be very sensitive to the geometry changes. Significant geometries change can be found in the S-PCT Cs series, which can't clearly differentiate the contribution on its aromaticity mainly from the symmetry breaking. Some more theoretical models are recommended here, the authors could introduce hydroxy- and sulfydryl-substituents to reduce the steric hindrance. And substituents on the parent PCT models without further relaxation are recommended for comparison.

Is the work clearly and accurately presented and does it cite the current literature?
Yes

Is the study design appropriate and does the work have academic merit?
Yes

Are sufficient details of methods and analysis provided to allow replication by others?
Yes

If applicable, is the statistical analysis and its interpretation appropriate?
Yes

Are all the source data underlying the results available to ensure full reproducibility?
Yes

Are the conclusions drawn adequately supported by the results?
Yes

Competing Interests: No competing interests were disclosed.

I confirm that I have read this submission and believe that I have an appropriate level of expertise to confirm that it is of an acceptable scientific standard.

Author Response 03 Mar 2022

Florian Glöcklhofer, Imperial College London, London, UK

Thank you for reviewing and approving our article and providing recommendations for further improvement. We would like to respond to these recommendations below. (Reviewer comments in italics)

- *More accurate concentration of the solution samples for the UV-Vis and PL measurements is recommended to be provided. Further discussion on their photoluminescent quantum yields instead of the comparison of the intensity would be more suitable for the discussion about the photophysics characters of the compounds.*

Response: The UV-vis and PL measurements were performed using 5 µM solutions in $CHCl_3$, as stated in the methods section. If the reviewer's comment is referring to "approx. 5 µM" in the caption of Figure 5, we would like to point out that "approx." was meant to reflect the limitations in accuracy when working with milligram quantities (despite using a high-precision balance). We have removed "approx." from the caption to avoid the impression that the concentration was not as accurate as possible. We appreciate the suggestion regarding the photoluminescence quantum yields (PLQYs). We have now determined the PLQYs of the macrocycles using quinine in 0.05 M H_2SO_4 as the reference to further support the conclusions of the article. Despite the observed increase in PL intensity upon introduction of the substituents, all three investigated macrocycles are still weak emitters; PLQYs of 0.06% for **PCT**, 0.65% for **O-PCT**, and 0.56% for **S-PCT** were determined. Due to the large difference in PLQY between the reference and the macrocycles, neutral density filters had to be used to enable PL measurements of the reference under the same instrument settings as used for the macrocycles. We believe this relative determination of the PLQYs can provide a good indication of the order of magnitude, but we suggest refraining from an overinterpretation of the exact values due to the potential sources of error in the determination. We have added the following sentence in the results and discussion section of the article and updated the conclusions and methods sections as well as the provided underlying research data accordingly: "Despite the increase in PL intensity upon introduction of the substituents, all three macrocycles are still weak emitters, with a relative determination of the photoluminescence quantum yield (PLQY) indicating values of <1% for **O-PCT** and **S-PCT** and <0.1% for **PCT**."

- *The chemical shift features as aromaticity criteria might be very sensitive to the geometry changes. Significant geometries change can be found in the S-PCT Cs series, which can't clearly differentiate the contribution on its aromaticity mainly from the symmetry breaking. Some more theoretical models are recommended here, the authors could introduce hydroxy- and sulfydryl-substituents to reduce the steric hindrance. And substituents on the parent PCT models without further relaxation are recommended for comparison.*

Response: We thank the reviewer for this suggestion. We have included computations on **O-PCT** and **S-PCT** based on a frozen **PCT** structure, see Table 1 and the ensuing discussion. Indeed, this procedure leads to similar NICS values as seen in the unsubstituted **PCT** molecule.

Competing Interests: No competing interests were disclosed.